

Construction of a Supramolecular Förster Resonance Energy Transfer System and Its Application Based on the Interaction between Cy3-Labeled Melittin and Phosphocholine Encapsulated Quantum Dots

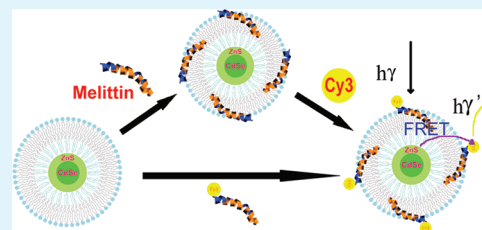
Yong-Qiang Dang, Hong-Wei Li, and Yuqing Wu*

State Key Laboratory of Supramolecular Structure and Materials, Jilin University, No. 2699, Qianjin Street, Changchun, 130012, China

S Supporting Information

ABSTRACT: Due to possessing unique optical properties, semiconductor quantum dots (QDs) have been applied to construct bioconjugates. Using QDs as donors, the Förster resonance energy transfer (FRET) system can be developed and applied to biological imaging and sensing, and various construction strategies have been reported. To provide a new practicable method, we introduce a protocol with two routes to construct a supramolecular FRET system based on the high-affinity interaction between melittin and phosphocholine. Melittin exists with a random coil structure in aqueous environments but will adopt a bent helix when inserted into natural or artificial membranes. Such specific and high affinity protein–membrane interaction makes it possible to construct a QDs-based FRET system. The strategy applying protein–membrane interaction to construct a QDs-based FRET system can be applied to the investigation on the protein–membrane interaction through distance-depended FRET and further proteolysis of trypsin. Because of the existence of various protein–membrane interactions in real life, the system has the potential to be expanded to other related systems.

KEYWORDS: Förster resonance energy transfer, quantum dots, protein–membrane interaction, phosphocholine, melittin, protease, trypsin



1. INTRODUCTION

Förster resonance energy transfer (FRET), the nonradiative transfer of energy from a fluorescent donor to an acceptor chromophore via a dipole–dipole coupling mechanism, is a powerful tool in the fields of biology, biochemistry, medicine, and other life sciences.^{1,2} Due to FRET depending on the r^{-6} distance, it can determine the distance between two fluorochromes in a distance range of 1–10 nm,³ and it has been applied in the determination of concentrations⁴ and structural changes of molecular systems within nanometer-scale systems in vitro and in vivo.⁵ Several applications on FRET-based biosensors for functional intracellular investigations and cellular imaging have also been developed recently.^{6–8} Quantum dots (QDs) are excellent FRET donors because of their capacity to bind multiple acceptor molecules and unique photophysical properties, such as high quantum yields, narrow fluorescence spectra, tunable fluorescence wavelength, and high resistance to photodegradation.^{9,10} Recent reports have described the approaches using QDs as a FRET donor with organic fluorophores, organic quenchers, or gold nanoparticles as the acceptor.^{11,12}

The strategy connecting donor and acceptor is important to the application of FRET. Using QDs as FRET donor, several methods have been designed to connect quantum dots with functional molecules. These include not only covalent couple^{13,14} and electrostatic attachment¹⁵ but also some specific

supramolecular interaction involving several weak interactions, such as the interactions between cDNA,^{16,17} between the Ni-NTA conjugate and oligohistidine-tagged proteins,^{18,19} between antigen and antibody, like biotin with streptavidin,^{20,21} and the host–guest complexation interaction between β -cyclodextrin and appropriate substrates²² and so on. Especially, the hexahistidine (His₆) segment to attach the peptide to the surface of the QDs via metal-affinity coordination interactions between His₆-tract and the metallic surface of the CdSe/ZnS core/shell QDs has been widely used to construct the FRET model to achieve the function of detecting enzymes.^{4,23–25} By introducing specific supramolecular interaction, FRET could be applied to more research areas. Herein, we report the introduction of the interaction between protein and membrane into the QDs-based FRET system.

Melittin is a widely used convenient model for exploring protein–membrane interactions.^{26–29} Such 26-residue peptide has a net positive charge of six at neutral pH, of which the N-terminal region (residues 1–20) is predominantly hydrophobic, whereas the C-terminal region (residues 21–26) is hydrophilic. The amphiphilic property of melittin results in a random coil structure in aqueous environments but adopts a bent helical

Received: October 27, 2011

Accepted: February 22, 2012

Published: February 22, 2012

conformation when inserted into natural or artificial membranes. While the C-terminal section is approximately parallel to the lipid bilayer, the N-terminal section is inserted halfway into the membrane.^{30,31} On the basis of such properties of melittin, the interaction between melittin and phospholipid is chosen to construct the FRET system. The specific and high affinity interaction between melittin and phosphocholine will provide a stable assembly which needs no extra assistance. The phosphocholine layer encapsulated on QDs provides a sphere scaffold to further binding with melittin. As the melittin can be easily incorporated into a recombinant protein, it can also be designed to deliver drug.³² These advantages make it possible to be applied to many other related research areas.

As a superfamily of enzymes, proteases play key functions in many normal biological processes.^{23,33} Trypsin, belonging to the protease, is the most important digestive enzyme produced by the pancreas. It participates in the transformation of many pancreatic proenzymes into their active forms in the intestine. Trypsin level is increased with several types of pancreatic diseases.^{34–36} Therefore, monitoring trypsin is directly important to clinical diagnosis and pharmaceutical drug development. In this study, we show not only the FRET applications on the distance determination of interaction between melittin and different kinds of phosphocholine, which is an important parameter to characterize the mechanism of membrane proteins, but also the application of such FRET system on the trypsin concentration assay. As various protein–membrane interactions exist in real life, different kinds of FRET systems would be designed through such similar supra-molecular strategy, which will expand the practical applications.

2. MATERIALS AND METHODS

2.1. Materials. CdSe/ZnS core/shell QDs with emission maxima centered at 525 nm are purchased from Wuhan Jiayuan Quantum Dots Company. Cy3 succinimidyl ester (Cy3-SE) is purchased from Fanbiochemicals Company. Melittin (89.4%) is purchased from Sigma-Aldrich (Shanghai) Trading Co., Ltd. DLPC and 1,2-dioleoyl-*sn*-glycero-3-phosphocholine (DOPC) are purchased from Avanti Polar Lipids, Inc. Trypsin (1:250) is purchased from Beijing Dingguochangsheng Biotechnology Co, Ltd.

2.2. Encapsulating Quantum Dots. QDs is encapsulated in DLPC (or DOPC) micelles^{37,38} as follows: 1 mL of CdSe/ZnS QDs in hexane (8 μ M, as supplied by the Corporation) is precipitated by addition of methanol (1 mL); then, the precipitate is dissolved in 1 mL of chloroform with 10 mg of DLPC (or DOPC). After complete evaporation of the chloroform, the residue is heated to and kept at 80 °C and then 1 mL water is added to obtain a suspension containing DLPC micelles, which include both empty micelles and those containing QDs. The empty micelles are removed with centrifugation at 12 000 rpm for 10 min, and the precipitate is washed by water for three times. Subsequently, the supernatant is discarded, and the DLPC encapsulated QDs (DLPC-TOPO-QDs) are resuspended in 1 mL of phosphate buffer solution (PBS, 5 mM, pH 8.0).

2.3. Cy3 Labeling on Melittin. One mg of melittin is dissolved in 1 mL of PBS solutions (5 mM, pH 8.0). Then, 1 equiv of Cy3 SE in 50 μ L of DMF is added, and the solution is stirred for 4 h at room temperature. Then, the solutions are dialyzed against PBS in a dialysis bag (MWCO 2000) to exclude the excessive Cy3. The final concentration of Cy3 in

labeling on melittin is determined by UV–vis absorption at 548 nm ($\epsilon = 150\,000$).³⁹

2.4. Förster Resonance Energy Transfer Analyses on Quantum Dots-Dye Construction. Fluorescence spectra are measured on a Shimadzu (Japan) RF-5301PC fluorescence spectrophotometer. Separate QDs and dye-acceptor emission profiles for each corresponding peptide/QDs ratio are gained through curve fitting using OriginLab (OriginLab Corp., Northampton, MA) by comparison to spectra collected from the individual component alone. FRET efficiency E_n (n is the number of dye-acceptors per QD) is determined using eq 1, where F_D and F_{DA} are the fluorescence intensities of the donor in the absence and presence of acceptor(s), respectively.

$$E = 1 - \frac{F_{DA}}{F_D} \quad (1)$$

Data from FRET efficiency is analyzed using Förster theory to determine the values for center-to-center (QD-to-dye) separation distance r using eq 2, where R_0 designates the Förster distance corresponding to 50% energy transfer efficiency for a single donor–single acceptor configuration. Equation 2 is applicable to single QD/multi-peptide dye conjugates as it specifically incorporates the presence of multiple acceptors centro-symmetrically arrayed around the QD donor.

$$r_n = R_0 \left(\frac{n(1 - E)}{E} \right)^{1/6} \quad (2)$$

2.5. Measurements of Fluorescence Lifetime. Fluorescence decay curves of the QDs are collected on a HORIBA JOBIN-YVON (French) FL3-TCSPC spectrophotometer. The sample is excited at 400 nm, and the fluorescence decay curves are collected at 530 nm.

2.6. Activity Assay of Trypsin. For the activity assay of trypsin, as-labeled Cy3-melittin is preincubated with different amounts of trypsin for 20 min at 37 °C in PBS (pH 8.0). Then, 0.2 equiv of DLPC-TOPO-QDs is added into such solution, and the sample is kept for 1 h at room temperature before collecting the fluorescence spectra. All assay points are performed in duplicate or triplicate, and finally, the standard deviations are shown.

3. RESULTS AND DISCUSSIONS

The CdSe/ZnS core/shell QDs, which are capped by trioctylphosphineoxide (TOPO), were encapsulated by DLPC first. When they are explored by transmission electron microscopy (TEM), the DLPC encapsulated QDs still appear fairly monodisperse without any aggregations (Figure S-1 in the Supporting Information). The comparison for the emission spectra of QDs before (TOPO-QDs) and after (DLPC-TOPO-QDs) being encapsulated by DLPC (Figure 1) shows that a minor red-shift ($\Delta\lambda = 5$ nm) of the emission peak is induced after encapsulation. Figure 1 also shows that the fluorescence emission of DLPC-TOPO-QDs and the absorption spectrum of Cy3-melittin have a remarkable spectral overlap, indicating the potential to produce efficient energy transfer from the QDs as a donor to the contiguous Cy3 dye as an acceptor. Then, we employ two routes to construct a FRET model based on the interaction between Cy3-labeled melittin and the DLPC encapsulated QDs (Scheme 1).

In the first route, we connect the DLPC-TOPO-QDs and the melittin without Cy3 labeling. As the fluorescence of intrinsic

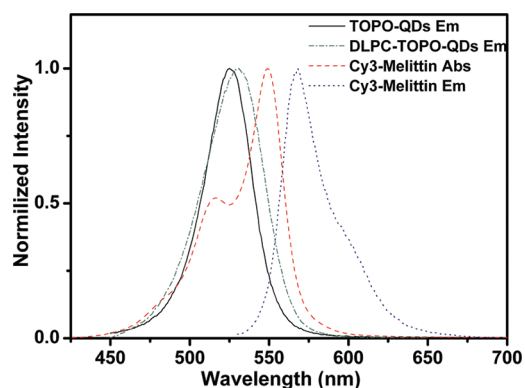


Figure 1. Normalized fluorescence emission spectra of the TOPO-QDs, DLPC-TOPO-QDs, and Cy3-melittin; together with the absorption spectra of Cy3-melittin.

tryptophan in melittin (Trp19) responds to the association of it to liposome bilayers,⁴⁰ we first use the fluorescence of Trp19 to characterize the interaction between melittin and the phosphocholine monolayer on QDs surface. The results manifest an obvious blue-shift after mixing the solutions of melittin and DLPC-TOPO-QDs (Figure 2A), which illustrate a change of Trp19 from bulk water to a hydrophobic membrane environment.⁴⁰ The fluorescence quenching of Trp19 may be attributed to the high absorption of QDs in this wavelength coverage (Figure S-2, Supporting Information). Therefore, we conjecture that the N-terminal section of melittin has inserted into the DLPC layer but the hydrophilic C-terminal section is still partially exposed to solution.

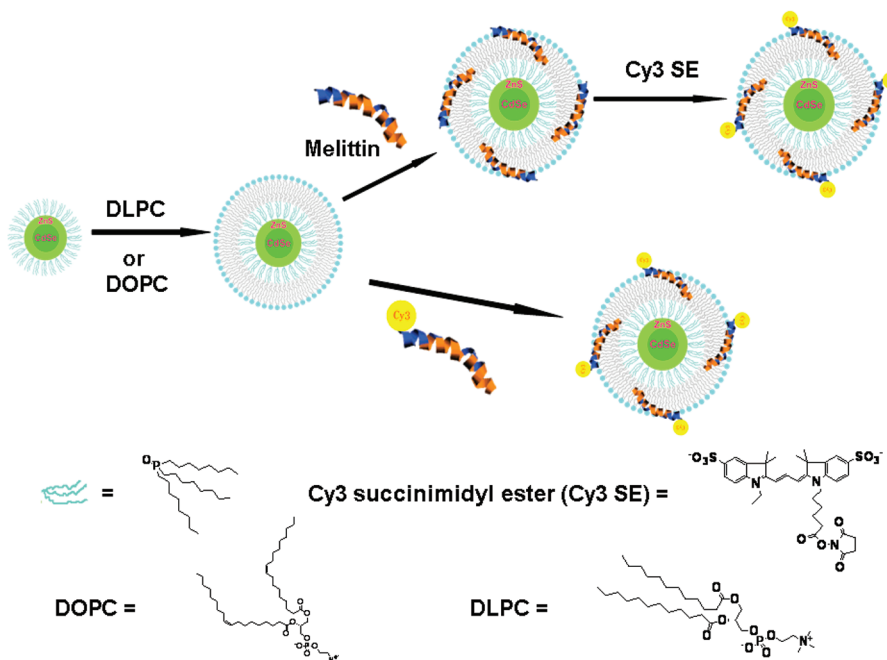
Then, the Cy3-SE is added into the solution containing the as-prepared DLPC-TOPO-QDs/melittin to label the exposed amino-group of melittin. A FRET between QDs and Cy3 is expected in this case. Figure 2B shows the fluorescence spectrum of the constructed DLPC-TOPO-QDs/melittin and those of it with time after Cy3-SE addition ($\lambda_{\text{ex}} = 400$ nm,

where the absorption of Cy3 is negligible). The fluorescence intensity of DLPC-TOPO-QDs decrease remarkably, and an obvious fluorescence emission band for Cy3 at 568 nm shows up with time. The observations clearly indicate that a FRET from the QDs to Cy3 takes place following the labeling of Cy3 on melittin. Furthermore, the control experiment under the same excitation ($\lambda_{\text{ex}} = 400$ nm), in which Cy3-SE is added directly into the DLPC-TOPO-QDs solution without melittin, does not exhibit such a Cy3 emission (Figure S-3, Supporting Information), supporting additionally that the observed FRET is ascribed to the interaction between Cy3-melittin and DLPC capsulated QDs.

The second route to construct FRET system between QDs and Cy3 is performed using Cy3 pre-labeled melittin (Cy3-melittin) to interact with DLPC-TOPO-QDs (the second route in Scheme 1). A 1 h incubation is necessary to bind the Cy3-melittin and DLPC-TOPO-QDs before collecting the fluorescence spectra. With the ratio increase of Cy3-melittin to DLPC-TOPO-QDs, the remarkable fluorescence quenching of DLPC-TOPO-QDs occurs simultaneously with the gradual increase of Cy3 emission at 568 nm (Figure 3A). After curve fitting, individual spectrum for DLPC-TOPO-QDs and Cy3-melittin are obtained and the FRET efficiency and relative photoluminescence (PL) signal of Cy3-melittin versus Cy3/QDs ratio is quantitatively calculated (Figure 3B). Similar changing tendency can be observed from both aspects of donor and acceptor with the increasing of Cy3/QDs ratio. Note that, among the molar ratios, the relative PL signal enhancement of acceptor is not as high as the FRET efficiency, being ascribed to the low quantum yield of Cy3 in PBS buffer solution ($\Phi=0.04$).⁴¹ That means that only a small proportion of energy transferred from QDs to Cy3 can be emitted.

To further verify that the quenches of QDs emission and the increase of Cy3 intensity are due to FRET, we measure the fluorescence lifetimes of the QDs emission before and after binding with Cy3-melittin (Figure 4). The fluorescence decay curve shows a much extended decay rate for the excited state of

Scheme 1. Preparation Schemes of Phosphocholine-TOPO-QDs/Cy3-Melittin Assembly in Two Different Routes



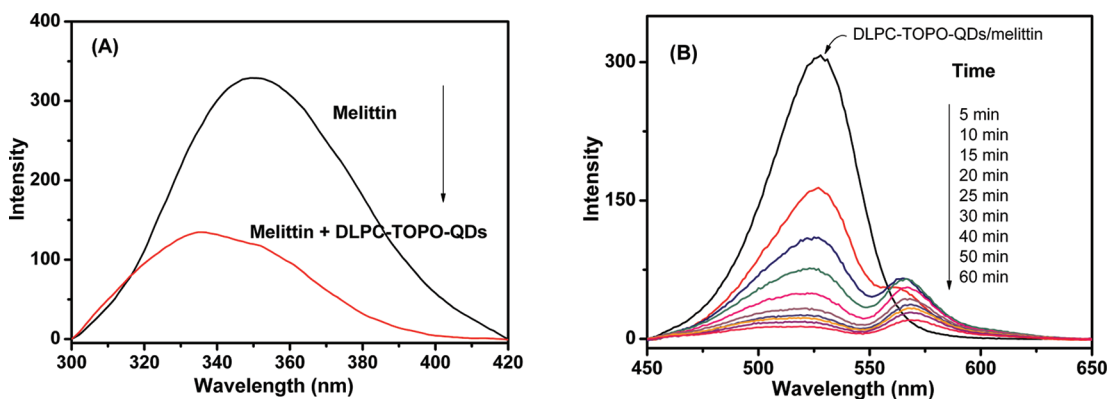


Figure 2. Fluorescence emission spectra of (A) the endogenous tryptophan in melittin ($10 \mu\text{M}$) before and after interacting with DLPC-TOPO-QDs ($1 \mu\text{M}$) for 1 h ($\lambda_{\text{ex}} = 280 \text{ nm}$) and (B) DLPC-TOPO-QDs/melittin and the time-course measurement after adding Cy3-SE ($10 \mu\text{M}$) ($\lambda_{\text{ex}} = 400 \text{ nm}$).

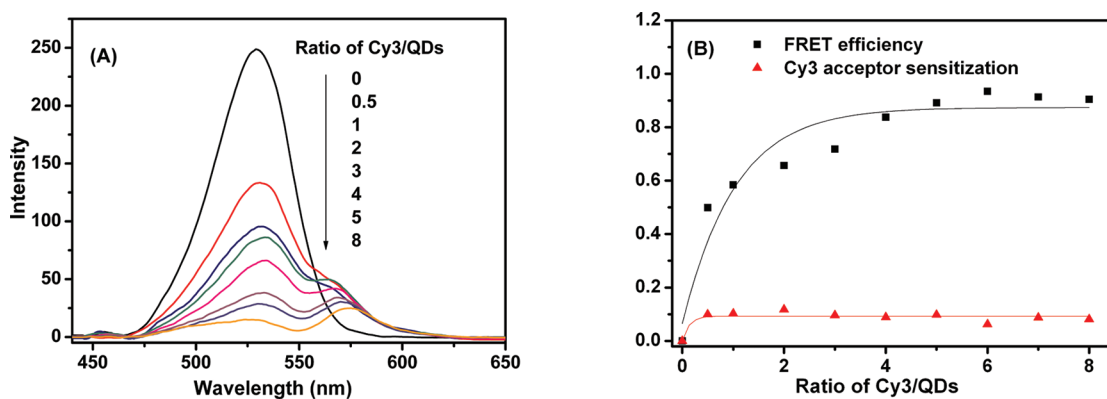


Figure 3. (A) Fluorescence spectra of DLPC-TOPO-QDs/Cy3-melittin with different ratio n of Cy3/QDs ($\lambda_{\text{ex}} = 400 \text{ nm}$). The contribution of direct excitation of Cy3 has been subtracted from the original fluorescence spectrum. (B) FRET efficiencies of DLPC-TOPO-QDs/Cy3-melittin deduce from the donor PL loss (square) and relative PL signal deduce from acceptor gain (triangle) as a function of Cy3-to-QD ratio (n).

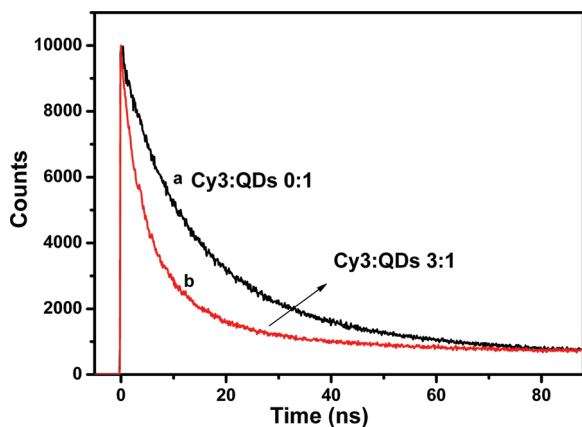


Figure 4. Fluorescence decay curves of the QDs emission at 530 nm ($\lambda_{\text{ex}} = 400 \text{ nm}$) for DLPC-TOPO-QDs in the absence and presence of 3 equiv of Cy3-melittin.

QDs after addition of Cy3-melittin. A fast component and a slow one are obtained after fitting the data,⁴² and both of them reduce (the fast one reduce from 8.9 to 3.8 ns and the slow one reduce from 25.6 to 15.9 ns), which should be ascribed to the energy transfer from QDs donor to Cy3 dye acceptor.

It is well-known that interactions of membrane proteins, peptide toxins, and delivery vectors with a lipid layer generally affect their fundamental activity strongly.^{43,44} FRET is one of

the most well-established techniques to monitor protein–membrane interactions, and the present FRET system could be a convenient model to study such interaction by changing the encapsulation layer or the membrane proteins. DLPC has shorter hydrophobic tails than DOPC, but DOPC has a double bond in the hydrophobic tails, which makes the length different between them. In addition, it was reported that melittin adopts different orientation in DLPC and DOPC membranes,⁴⁵ that might affect the inserting depth of melittin in membranes. Herein, we use DOPC instead of DLPC to encapsulate QDs and further compare the FRET differences of them between QDs and Cy3. The results in Figure 5 show that a slightly lower FRET efficiency is observed for DOPC-TOPO-QDs/Cy3-melittin in comparison to that of DLPC-TOPO-QDs/Cy3-melittin (Figure 3B). In addition, the center-to-center separation distance r between donor and acceptor are quantitatively calculated¹ on the basis of the FRET data for both of DLPC-TOPO-QDs/Cy3-melittin and DOPC-TOPO-QDs/Cy3-melittin systems, which reveal that the distance r is relatively shorter in DLPC-TOPO-QDs/Cy3-melittin ($5.7 \pm 0.3 \text{ nm}$) than in DOPC-TOPO-QDs/Cy3-melittin ($6.1 \pm 0.3 \text{ nm}$). More precise design and study would help to get more details of the interaction between lipid layer and membrane protein.

Several QDs-based FRET systems have been used for detecting the activities of enzymes^{24,46,47} by designing specific peptide modified on QDs. Herein, we show that our FRET

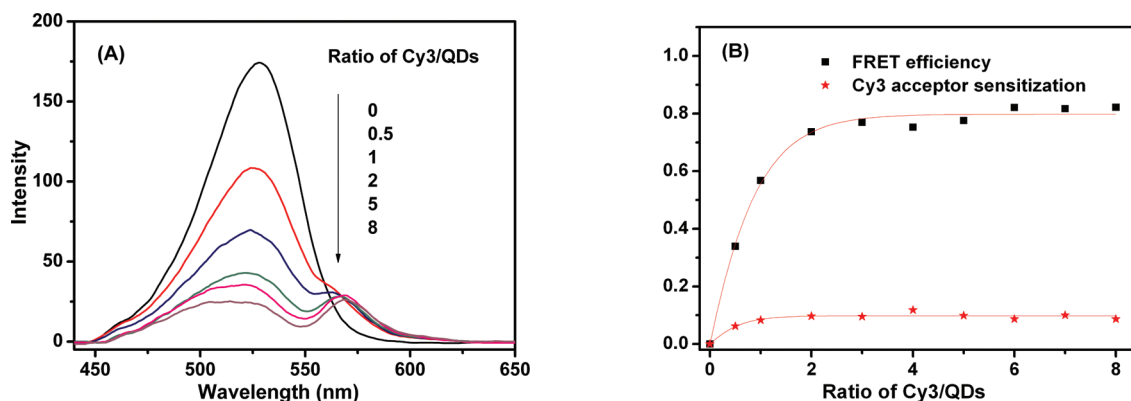


Figure 5. (A) Fluorescence spectra of DOPC-TOPO-QDs/Cy3-melittin with different ratio n of Cy3/QDs ($\lambda_{\text{ex}} = 400$ nm). (B) FRET efficiencies of DOPC-TOPO-QDs/Cy3-melittin (square) and DOPC-TOPO-QDs/Cy3-melittin (star) deduced from the donor PL loss as a function of Cy3/QD ratio (n).

system also has the capacity to detect trypsin activity. Since trypsin cleavage of peptidyl sequences on the side of lysine (K) and arginine (R) residues³⁴ and melittin meets this condition, we expect that trypsin will hydrolyze melittin and destroy the interaction between DLPC-TOPO-QDs and Cy3-melittin, demolishing the FRET between QDs and Cy3. Actually, exposing the preassembled DLPC-TOPO-QDs/Cy3-melittin complex (5:1 mol ratio of Cy3/QDs) to different amounts of trypsin for 1 h incubation, little to no fluorescence recovery of QDs can be observed. Sapsford et al. have demonstrated that the protease could be sterically precluded from productive interactions with the peptide substrate once assembled on the QDs,⁴¹ so we suggest a similar steric effect resulting in noneffective proteolysis of melittin by trypsin. Then, we change the protocol to incubate Cy3-melittin with trypsin for 20 min at 37 °C first and then add the DLPC-TOPO-QDs and allow them to assemble for 1 h. The collected data show that the presence of trypsin induces remarkable changes of FRET. By converting the changes in QDs donor PL to I/I_0 (relative to DLPC-TOPO-QDs/Cy3-melittin complex not exposed to trypsin), we plot the dose response increase of QDs PL against trypsin concentration (Figure 6). The result is a direct evidence of the peptide cleavage by trypsin; it implies not only that the following comeback of QDs fluorescence induced by trypsin cleavage on melittin definitely can be used to assay its protease activity but also that the response of DLPC-TOPO-QDs/Cy3-melittin to trypsin could be further applied to the high-

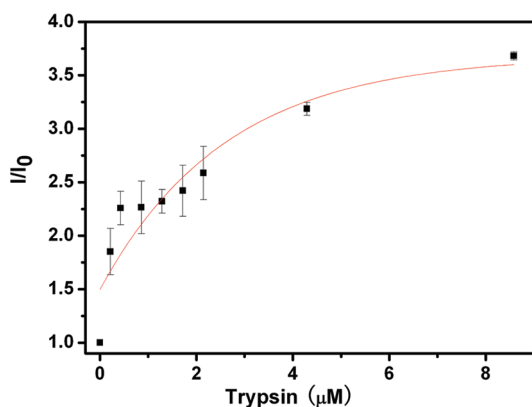


Figure 6. Increasing plot of QDs PL (I/I_0) as a function of trypsin concentration.

throughput screening of trypsin inhibitors, which are carried out currently.

4. CONCLUSIONS

The high affinity interaction between phosphocholine and melittin is used to modify CdSe/ZnS core/shell QDs, and a FRET system between QDs and Cy3 labeling on melittin is formed, which is assayed by steady-state photoluminescence spectra and the time-resolved fluorescence spectra. Such an efficient FRET system is used to characterize the center-to-center separation distance r between donor and acceptor, which can be applied to study the protein–membrane interactions, monitor the proteolytic activity of trypsin, and further have the potential to be used in the high-throughput screening of trypsin inhibitors. Such a concept and protocol in constructing a QDs-based FRET system based on the specific interaction between membranes and melittin will have more applications because of the wide existence of protein–membrane interactions.

■ ASSOCIATED CONTENT

Supporting Information

The TEM image of the TOPO-QDs and DLPC-TOPO-QDs. Normalized absorption spectra of TOPO-QDs. Fluorescence emission spectra of the DLPC-TOPO-QDs and time-course measurement after adding Cy3-SE. This material is available free of charge via the Internet at <http://pubs.acs.org>.

■ AUTHOR INFORMATION

Corresponding Author

*Fax: +86-431-85193421. Tel: +86-431-85168730. E-mail: yqwu@jlu.edu.cn.

Notes

The authors declare no competing financial interest.

■ ACKNOWLEDGMENTS

The present work is supported by the projects of the NSFC (Nos. 20934002, 21003061, and 20973073), Jilin Province Natural Science Foundation (20070926-01), the National Basic Research Program (2007CB808006), and the State Key Laboratory of Supramolecular Structure and Materials, Jilin University. The authors also thank Ms. Meghan K. Hatfield, an exchange undergraduate student from the University of West Virginia, for English correction.

■ REFERENCES

- (1) Clapp, A. R.; Medintz, I. L.; Mauro, J. M.; Fisher, B. R.; Bawendi, M. G.; Mattoussi, H. *J. Am. Chem. Soc.* **2004**, *126*, 301–310.
- (2) Qin, B.; Chen, H.; Liang, H.; Fu, L.; Liu, X.; Qiu, X.; Liu, S.; Song, R.; Tang, Z. *J. Am. Chem. Soc.* **2010**, *132*, 2886–2888.
- (3) Morgner, F.; Geissler, D.; Stufler, S.; Butlin, N. G.; Lohmannsroben, H. G.; Hildebrandt, N. *Angew. Chem., Int. Ed.* **2010**, *49*, 7570–7574.
- (4) Dennis, A. M.; Bao, G. *Nano Lett.* **2008**, *8*, 1439–1445.
- (5) Gambin, Y.; Deniz, A. A. *Mol. BioSyst.* **2010**, *6*, 1540–1547.
- (6) Jares-Erijman, E. A.; Jovin, T. M. *Nat. Biotechnol.* **2003**, *21*, 1387–1395.
- (7) Ding, Y.; Ai, H.-w.; Hoi, H.; Campbell, R. E. *Anal. Chem.* **2011**, *83*, 9687–9693.
- (8) Richards, C. I.; Hsiang, J.-C.; Khalil, A. M.; Hull, N. P.; Dickson, R. M. *J. Am. Chem. Soc.* **2010**, *132*, 6318–6323.
- (9) Algar, W. R.; Tavares, A. J.; Krull, U. J. *Anal. Chim. Acta* **2010**, *673*, 1–25.
- (10) Meng, H.; Yang, Y.; Chen, Y.; Zhou, Y.; Liu, Y.; Chen, X. a.; Ma, H.; Tang, Z.; Liu, D.; Jiang, L. *Chem. Commun.* **2009**, 2293–2295.
- (11) Suzuki, M.; Husimi, Y.; Komatsu, H.; Suzuki, K.; Douglas, K. T. *J. Am. Chem. Soc.* **2008**, *130*, 5720–5725.
- (12) Quach, A. D.; Crivat, G.; Tarr, M. A.; Rosenzweig, Z. *J. Am. Chem. Soc.* **2011**, *133*, 2028–2030.
- (13) Prasuhn, D. E.; Feltz, A.; Blanco-Canosa, J. B.; Susumu, K.; Stewart, M. H.; Mei, B. C.; Yakovlev, A. V.; Loukou, C.; Mallet, J.-M.; Oheim, M.; Dawson, P. E.; Medintz, I. L. *ACS Nano* **2010**, *4*, 5487–5497.
- (14) Freeman, R.; Finder, T.; Gill, R.; Willner, I. *Nano Lett.* **2010**, *10*, 2192–2196.
- (15) Ho, Y. P.; Chen, H. H.; Leong, K. W.; Wang, T. H. *J. Controlled Release* **2006**, *116*, 83–89.
- (16) Zhang, C. Y.; Yeh, H. C.; Kuroki, M. T.; Wang, T. H. *Nat. Mater.* **2005**, *4*, 826–831.
- (17) Liu, J.; Lee, J. H.; Lu, Y. *Anal. Chem.* **2007**, *79*, 4120–4125.
- (18) Susumu, K.; Medintz, I. L.; Delehanty, J. B.; Boeneman, K.; Mattoussi, H. *J. Phys. Chem. C* **2010**, *114*, 13526–13531.
- (19) Kwon, H.; Hong, S.; Kim, H.; Choi, Y.; Kim, J.; Song, R. *Chem. Commun.* **2010**, *46*, 8959–8961.
- (20) Pathak, S.; Davidson, M. C.; Silva, G. A. *Nano Lett.* **2007**, *7*, 1839–1845.
- (21) Boeneman, K.; Deschamps, J. R.; Buckhout-White, S.; Prasuhn, D. E.; Blanco-Canosa, J. B.; Dawson, P. E.; Stewart, M. H.; Susumu, K.; Goldman, E. R.; Ancona, M.; Medintz, I. L. *ACS Nano* **2010**, *4*, 7253–7266.
- (22) Freeman, R.; Finder, T.; Bahshi, L.; Willner, I. *Nano Lett.* **2009**, *9*, 2073–2076.
- (23) Sapsford, K. E.; Farrell, D.; Sun, S.; Rasooly, A.; Mattoussi, H.; Medintz, I. L. *Sens. Actuators, B* **2009**, *139*, 13–21.
- (24) Ghadiali, J. E.; Lowe, S. B.; Stevens, M. M. *Angew. Chem., Int. Ed.* **2011**, *50*, 3417–3420.
- (25) Biswas, P.; Cella, L. N.; Kang, S. H.; Mulchandani, A.; Yates, M. V.; Chen, W. *Chem. Commun.* **2011**, *47*, 5259–5261.
- (26) Fernandez-Vidal, M.; White, S. H.; Ladokhin, A. S. *J. Membr. Biol.* **2011**, *239*, 5–14.
- (27) Torrens, F.; Castellano, G.; Campos, A.; Abad, C. *J. Mol. Struct.* **2007**, *834*, 216–228.
- (28) Stromstedt, A. A.; Wessman, P.; Ringstad, L.; Edwards, K.; Malmsten, M. *J. Colloid Interface Sci.* **2007**, *311*, 59–69.
- (29) Hall, K.; Lee, T. H.; Aguilar, M. I. *J. Mol. Recognit.* **2011**, *24*, 108–118.
- (30) Terwilliger, T. C.; Eisenberg, D. *J. Biol. Chem.* **1982**, *257*, 6016–6022.
- (31) Niemz, A.; Tirrell, D. A. *J. Am. Chem. Soc.* **2001**, *123*, 7407–7413.
- (32) Soman, N. R.; Lanza, G. M.; Heuser, J. M.; Schlesinger, P. H.; Wickline, S. A. *Nano Lett.* **2008**, *8*, 1131–1136.
- (33) Grant, S. A.; Weillbaecher, C.; Lichlyter, D. *Sens. Actuators, B* **2007**, *121*, 482–489.
- (34) Xue, W.; Zhang, G.; Zhang, D.; Zhu, D. *Org. Lett.* **2010**, *12*, 2274–2277.
- (35) Xu, K.; Liu, F.; Ma, J.; Tang, B. *Analyst* **2011**, *136*, 1199–1203.
- (36) Zhu, Q.; Zhan, R.; Liu, B. *Macromol. Rapid Commun.* **2010**, *31*, 1060–1064.
- (37) Dubertret, B.; Skourides, P.; Norris, D. J.; Noireaux, V.; Brivanlou, A. H.; Libchaber, A. *Science* **2002**, *298*, 1759–1762.
- (38) Skajaa, T.; Zhao, Y.-M.; van den Heuvel, D. J.; Gerritsen, H. C.; Cormode, D. P.; Koole, R.; van Schooneveld, M. M.; Post, J. A.; Fisher, E. A.; Fayad, Z. A.; Donega, C. d. M.; Meijerink, A.; Mulder, W. J. M. *Nano Lett.* **2010**, *10*, 5131–5138.
- (39) Mujumdar, R. B.; Ernst, L. A.; Mujumdar, S. R.; Lewis, C. J.; Waggoner, A. S. *Bioconjugate Chem.* **1993**, *4*, 105–111.
- (40) Surewicz, W. K.; Epand, R. M. *Biochemistry* **1984**, *23*, 6072–6077.
- (41) Sapsford, K. E.; Granek, J.; Deschamps, J. R.; Boeneman, K.; Blanco-Canosa, J. B.; Dawson, P. E.; Susumu, K.; Stewart, M. H.; Medintz, I. L. *ACS Nano* **2011**, *5*, 2687–2699.
- (42) Javier, A.; Magana, D.; Jennings, T.; Strouse, G. F. *Appl. Phys. Lett.* **2003**, *83*, 1423–1425.
- (43) Postupalenko, V. Y.; Shvadchak, V. V.; Duportail, G.; Pivovarenko, V. G.; Klymchenko, A. S.; Mely, Y. *Biochim. Biophys. Acta* **2011**, *1808*, 424–432.
- (44) Wimley, W. C.; White, S. H. *Biochemistry* **2000**, *39*, 161–170.
- (45) Haldar, S.; Raghuraman, H.; Chattopadhyay, A. *J. Phys. Chem. B* **2008**, *112*, 14075–14082.
- (46) Ghadiali, J. E.; Cohen, B. E.; Stevens, M. M. *ACS Nano* **2010**, *4*, 4915–4919.
- (47) Boeneman, K.; Mei, B. C.; Dennis, A. M.; Bao, G.; Deschamps, J. R.; Mattoussi, H.; Medintz, I. L. *J. Am. Chem. Soc.* **2009**, *131*, 3828–3829.